Journal of Engineering and Technology for Industrial Applications

ISSN ONLINE: 2447-0228

ITEGAM-JETIA

Manaus, v.12 n.57, p. 408-415. January/February, 2026.

DOI: https://doi.org/10.5935/jetia. v12i57.3027

RESEARCH ARTICLE OPEN ACCESS

OPTIMAL CONVERSION TOPOLOGIES FOR GRID-CONNECTED PV SYSTEMS: A COMPARATIVE STUDY OF SINGLE-STAGE AND TWO-STAGE CONFIGURATIONS

Abdelmoumen Ghilani[1], Amel Terki[2], Ahmed Marouane Ghodbane[3]
Zakaria Alili[4] and Oussama Belaroussi[5]

[1]LMSE Laboratory of Energy Systems Modeling, Department of Electrical Engineering, University of Biskra- Biskra 07000, Algeria
[2, 3, 5]LGEB Laboratory, Department of Electrical Engineering, University of Biskra- Biskra 07000, Algeria
[4]LEE Laboratory, University of Msila, Department of Electrical Engineering- Msila 28000, Algeria

[1]https://orcid.org/0009-0008-3522-9696, [2]https://orcid.org/0009-0001-6633-0761, [3]https://orcid.org/0009-0004-5028-116X
[4]https://orcid.org/0009-0008-3704-0897, [5]https://orcid.org/0000-0003-1777-4187

Email: abdelmoumen.ghilani@univ-biskra.dz , a.terki@univ-biskra.dz, marouane.ghodbane@univ-biskra.dz , Zakaria.alili@univ-msila.dz , oussama.belaroussi.47@gmail.com

ARTICLE INFO

Article History
Received: November 30, 2025
Revised: December 10, 2025
Accepted: January 1, 2026
Published: January 31, 2026

Keywords:
Single stage,
Two stage,
PV Grid connected,
MPPT,
Incremental conductance,
Renewable Energy.

ABSTRACT

With the ongoing rise in global energy demand, grid-connected photovoltaic (PV) systems are increasingly recognised as a viable and sustainable energy alternative. These systems primarily operate using one of two distinct topologies: the two-stage (DC-DC-AC) configuration, in which the voltage from solar panels is initially boosted by a DC-DC converter before being converted to AC through an inverter. While functional, this design presents inherent drawbacks, including increased system size, higher costs, and reduced efficiency due to multiple conversion stages. To address these challenges, the single-stage (DC-AC) topology has been developed, directly linking solar panels to the inverter and eliminating the need for a DC-DC converter to enhance overall system efficiency. This study aims to identify the optimal topology for grid-connected PV systems by offering a comprehensive comparative analysis of power loss, system efficiency, and MPPT algorithm performance across these two configurations in a 150 kW grid-connected PV system under varying irradiance conditions. The simulation results underscore the superiority of the single-stage topology, demonstrating its streamlined design, cost-efficiency, and improved energy performance. Consequently, this analysis provides a valuable framework for engineers and researchers in selecting optimised configurations for grid-connected PV systems.

I. INTRODUCTION

Due to the increasing global need for electrical energy, solar photovoltaic (PV) technology is recognised as a cost-effective solution for power generation across various sectors, including residential energy systems, small off-grid applications, and large infrastructure projects [1]. The power output of photovoltaic panels must be controlled, as it depends on external conditions such as temperature and solar irradiation. Maximum Power Point Tracking (MPPT) techniques are used to ensure that PV panels produce the maximum possible power [2]. Incremental Conductance (IncCond) and Perturb and Observe (P&O) are two of the most extensively utilised algorithms for grid-connected systems, owing to their clarity and simplicity of implementation [3]. Grid-connected PV systems use two topologies. The first is a two-stage topology, as shown in Figure 1, which uses a DC-DC converter to boost the photovoltaic voltage and track the maximum power point of the solar panels. In the second stage, a single-phase or three-phase inverter injects the electricity produced by the solar PV system into the grid and ensures its synchronization [4].

The two-stage topology has certain drawbacks, despite its benefits in controller design. Additional stages increase system complexity, which reduces overall system dependability [5]. As the number of circuit stages increases, power losses also increase, lowering the overall efficiency of energy transfer. As shown in Figure 2, a system that relies solely on the inverter is known as a single-stage topology. It is designed to eliminate the drawbacks of the two-stage topology [6].

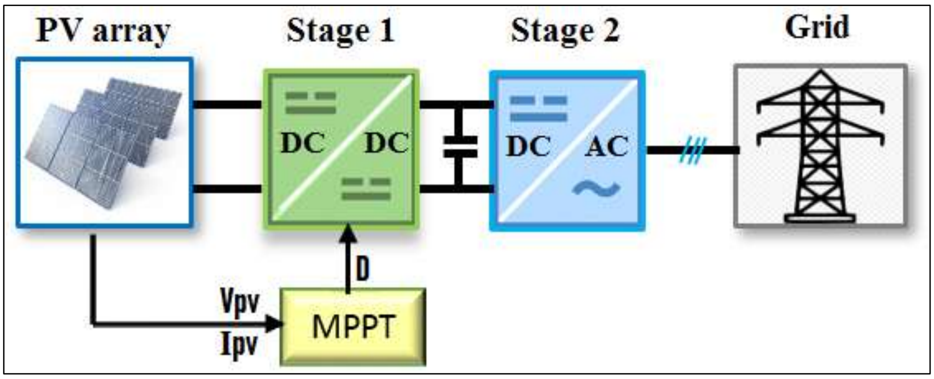

Figure 1: Two stage structure.
Source: Authors, (2026).

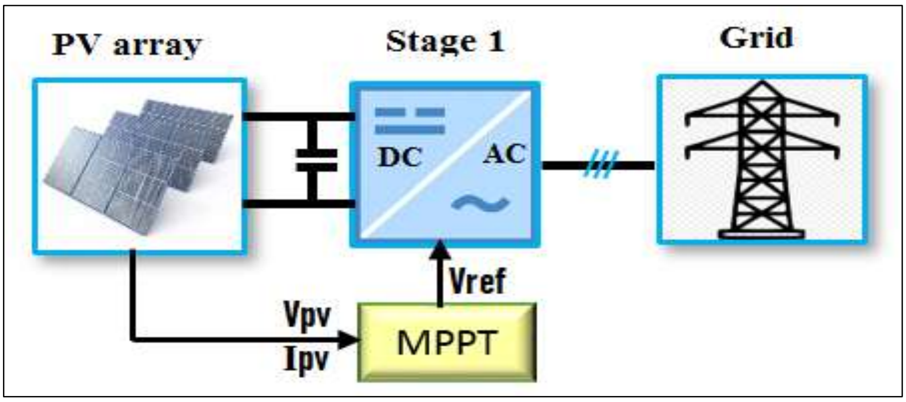

Figure 2: Single stage structure.
Source: Authors, (2026).

The primary objective of this paper is a comparative study of system efficiency, power loss, and the performance of Maximum Power Point Tracking (MPPT) methods between single-stage and two-stage topologies for a 150 kW solar photovoltaic (PV) power plant. This study provides valuable insights to support informed decision-making in the design and implementation of grid-connected PV systems. The paper is organised as follows: Section 2 details the design of the solar PV array. Section 3 discusses the modelling of the DC-DC boost converter. Section 4 describes the MPPT methods used in the analysis. In Section 5, the control technique of the grid-connected inverter is explained. Section 6 presents the simulation process and compares the results obtained. Finally, Section 7 concludes the study by summarising the key findings and their implications.

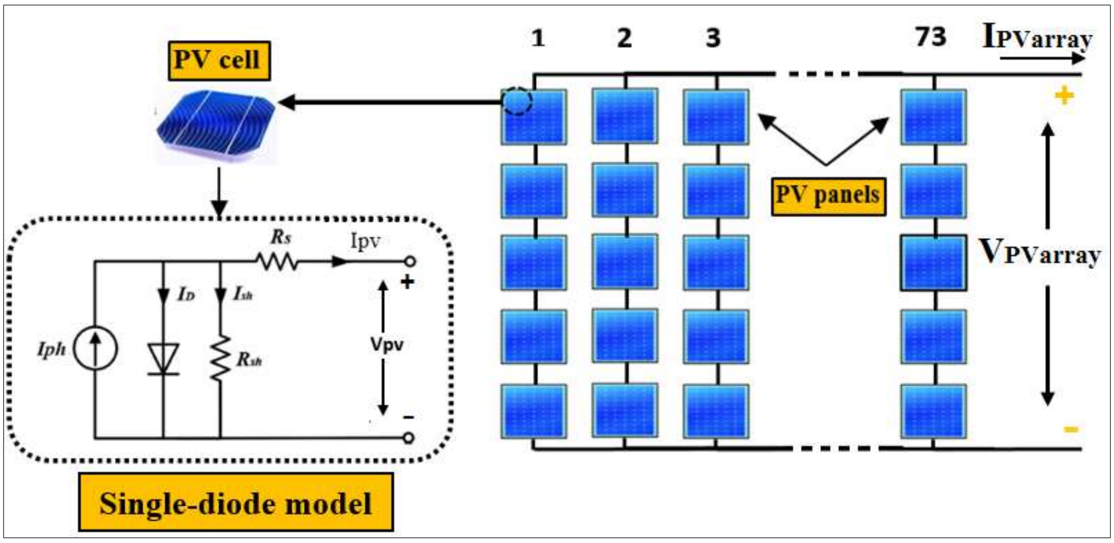

Figure 3: The PV array configuration.
Source: Authors, (2026).

II. PV POWER PLANT MODELING AND SIZING

The PV array represents the entire energy-generating system[7], consisting of multiple modules connected in series or parallel to produce high levels of current, voltage, and power. In this study, the PV system includes 365 solar panels arranged into 73 strings, with each string containing five panels. Table 1 outlines the characteristics of the PV modules under standard test conditions (STC).

Table 1: PV module characteristics.

The Parameter	The Value
Rated maximum power (P_{max})	415 W
Voltage at P_{max}	72.9 V
Current at P_{max}	5.69 A
Open-circuit PV voltage	85.3 V
Short-circuit PV current	6.09 A
The number of cells	128

Source: Authors, (2026).

Figure 3 displays the PV array design with the single-diode model, which is frequently used to study the behavior and performance of PV cells [8]. The I_{PV} can be determined by using the following equation[9]:

$$I_{PV} = I_{ph} - I_0\left[exp^{\frac{V_{pv}+I_{pv}R_s}{\alpha V_t}} - 1\right] - \frac{V_{pv} + I_{pv}R_s}{R_{sh}} \quad (1)$$

In this equation, I_{PV} represents the PV output current, and V_{PV} denotes the PV output voltage. The parameters include R_{sh} the shunt resistance, and R_s, the series resistance. I_{ph} is the current generated by solar irradiation, while V_t refers to the thermal voltage. Additionally, I_0 is the diode saturation current, and α stands for the ideality factor of the junction[3].

Figures 4 and 5 display the characteristics of the photovoltaic power plant under varying solar irradiance levels of 300, 600, 800, and 1000 W/m². These figures illustrate how irradiance affects key performance metrics, including output voltage (V_{PV}), power (P_{PV}), and current (I_{PV}).

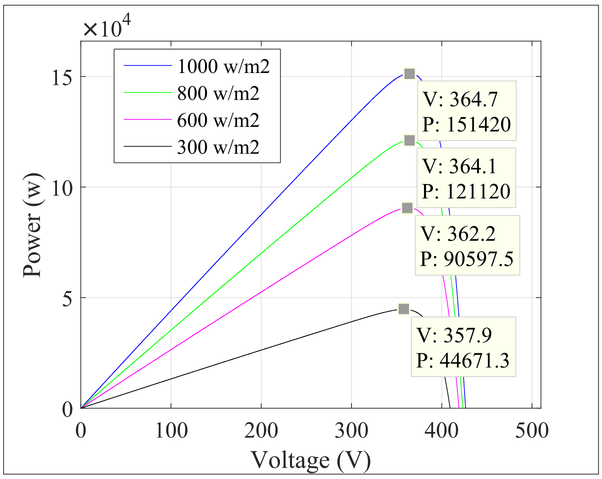

Figure 4: The power-voltage characteristic curve.
Source: Authors, (2026).

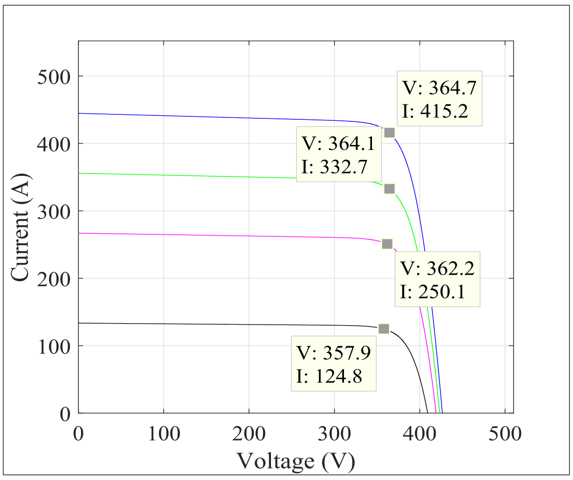

Figure 5: The current-voltage characteristic curve.
Source: Authors, (2026).

At maximum irradiance (1000 W/m²), the PV system achieves a voltage of 364.7 V with a power output of 151.42 kW, and a corresponding current of 415.2 A. As irradiance decreases to 800 W/m², the system voltage remains relatively stable at 364.1 V, but power and current reduce to 121.12 kW and 332.7 A, respectively. At 600 W/m², the voltage is 362.2 V, power output is 90.60 kW, and current is 250.1 A. Lastly, under the lowest irradiance of 300 W/m², the voltage drops slightly to 357.9 V, with power output at 44.67 kW and current at 124.8 A.

III. MODELLING OF THE DC–DC BOOST CONVERTER

The Boost Converter, as shown in Figure 6, consists of key components including an inductor, a power switch (typically a MOSFET or IGBT), a diode, and input/output capacitors for voltage filtering [10]. These components work together to boost the input voltage to a higher output level. In this system, the Maximum Power Point Tracking (MPPT) algorithm dynamically adjusts the converter's duty cycle (D) to continuously track the Maximum Power Point (MPP) of the PV array, optimizing power extraction under varying irradiance conditions [11]. The relationship between the output voltage (V_{out}) and input voltage (V_{pv}) is represented by the following equation [12]:

$$V_{out} = \frac{V_{pv}}{1 - D} \quad (2)$$

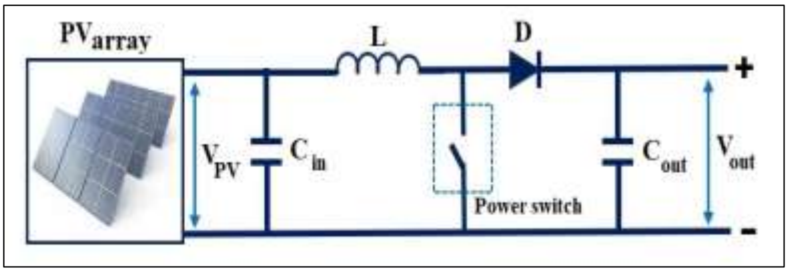

Figure 6: DC-DC boost converter.
Source: Authors, (2026).

To design the boost converter for efficient elimination of current and voltage ripples, the following equations are used [13]:

$$C_{in} = \frac{D}{8 \times f^2 \times L \times 0.1} \tag{3}$$

$$L = \frac{D(1-D)^2 \times R}{2 \times f} \tag{4}$$

$$R = \frac{P_{MPP}}{V_{grid}} \tag{5}$$

IV. INCREMENTAL CONDUCTANCE MPPT ALGORITHM

This algorithm is based on the slope of the PV system's voltage and power curvese is zero at the Maximum Power Point (MPP) [14], allowing the MPP to be tracked by comparing the incremental conductance ($\frac{\Delta I}{\Delta v}$) to the instantaneous conductance ($\frac{I}{v}$), as shown in Equation 6 [15]. This comparison indicates which side of the MPP the PV array is currently operating on[16] . Figure 7 the flowchart of the Incremental Conductance (IncCond) method.

$$\frac{dp}{dv} = \frac{dVI}{dv} = I + V\frac{\Delta I}{\Delta v} \tag{6}$$

$$\frac{\Delta I}{\Delta v}\begin{cases} = \frac{-I}{v} \ At\ MPP \\ > \frac{-I}{v} \ Left\ of\ MPP \\ < \frac{-I}{v} \ Right\ of\ MPP \end{cases} \tag{7}$$

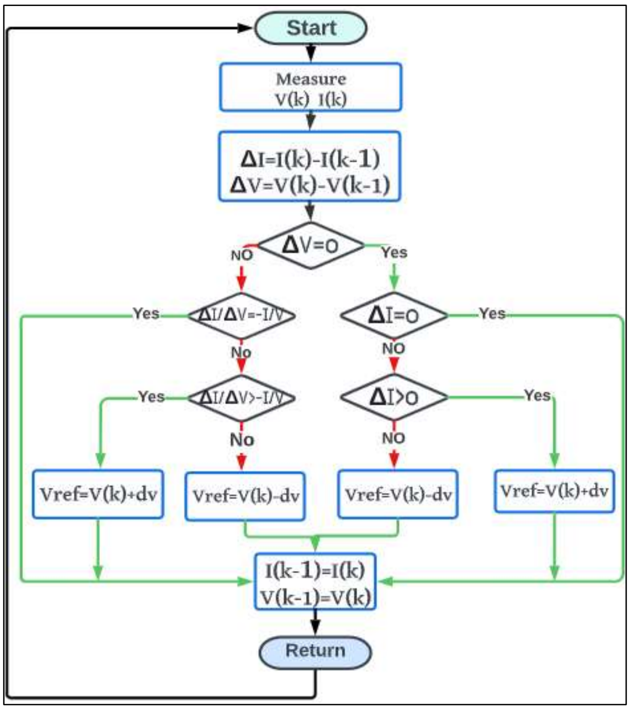

Figure 7: Flow chart of IncCond Method.
Source: Authors, (2026).

V. CONTROL STRATEGY OF PV INVERTER

The control strategy for the PV inverter consists of two main control loops. The first loop employs a proportional-integral (PI) controller to maintain the DC-link voltage at either the nominal reference voltage or the maximum power point (MPP) voltage[17], as determined by the MPPT algorithm in a single-stage configuration. The output of this loop is the reference for the active current. Meanwhile, the reactive current reference is typically set to zero to achieve a power factor close to unity[10].

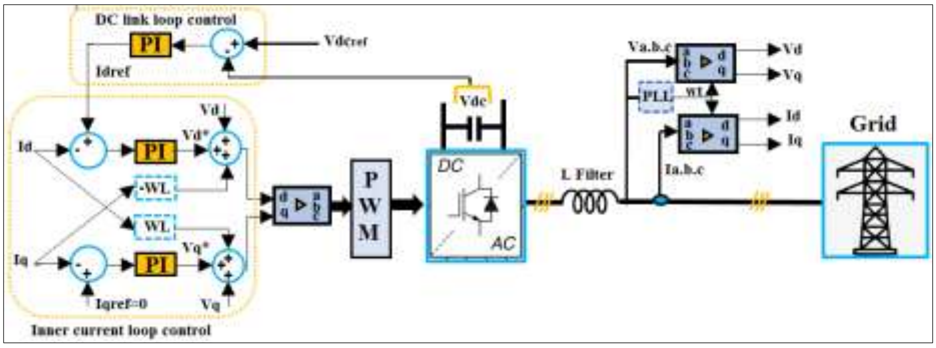

Figure 8: Control structure of the three-phase inverter.
Source: Authors, (2026).

To synchronise the inverter's output with the grid, a phase-locked loop (PLL) is used [18]. The PLL provides the phase angle required for the park transformation, which converts the grid's three-phase instantaneous voltages and currents into the dq reference frame[19]. Within this frame, inner PI controllers generate active and reactive voltage references based on the desired power output[20]. The dq-to-abc transformation then uses these active and reactive voltage references to create a reference voltage, Vabc, which is fed into the PWM generator. This generator produces the switching pulses for the inverter[4]. Figure 8 illustrates the concept of dq-control for a three-phase PV inverter.

VI. SIMULATION RESULTS AND DISCUSSION

In this section, for comparison, the performances of the two topologes. The simulations shown in Figures 9 and 10 are run, and their parameters are listed in Table 2.

Table 1: Simulation parameters.

The Parameter	The Value
U_{grid}	220 V
frequency	50 Hz
L_{Filter} , R_{Filter}	0.09 H 1.1Ω
L_{boost}	3 mH
C_{boost}	1100 µF
C_{DC}	120000 μF

Source: Authors, (2026).

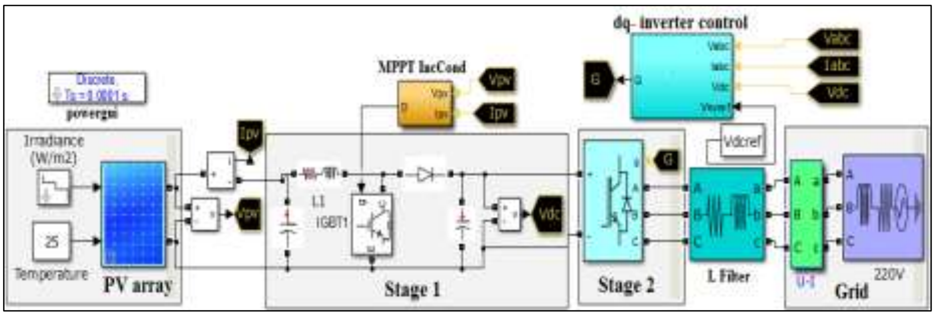

Figure 9: Simulation model of the two-stage topology.
Source: Authors, (2026).

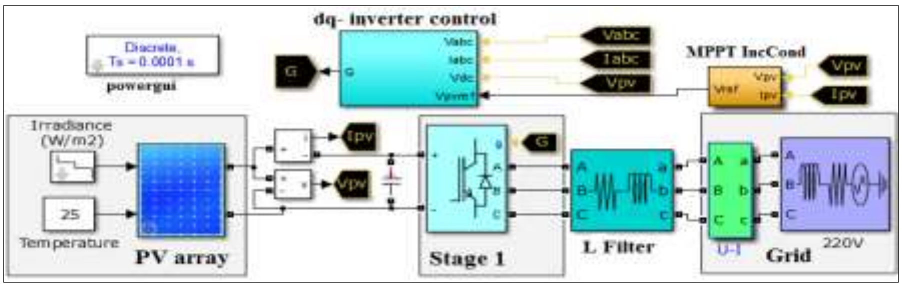

Figure 10: Simulation model of the single-stage topology.
Source: Authors, (2026).

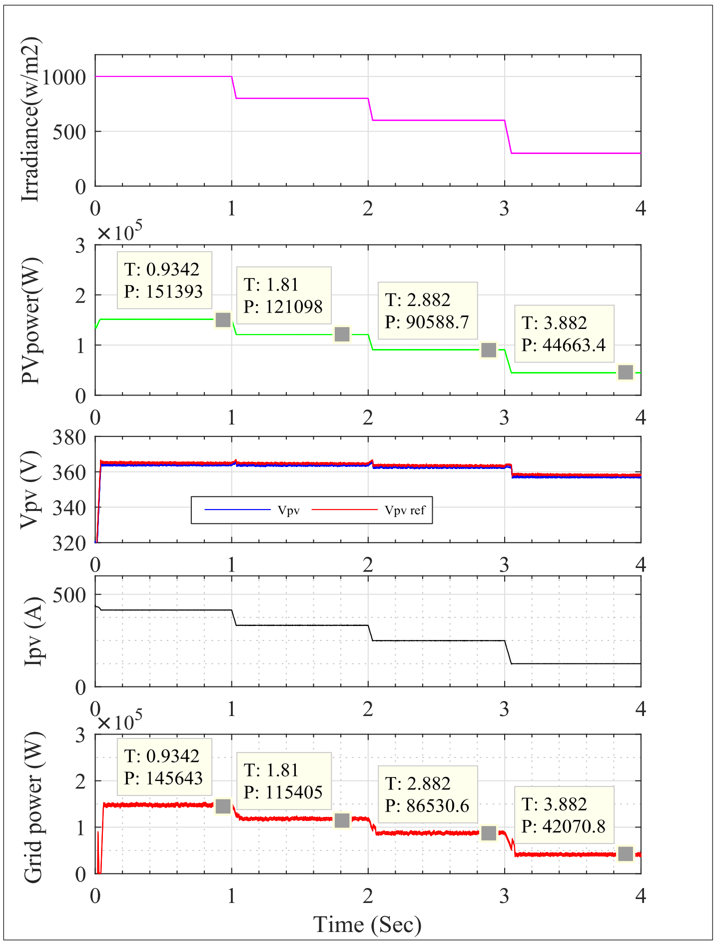

Figure 11 : Single-stage topologies Simulation result.
Source: Authors, (2026).

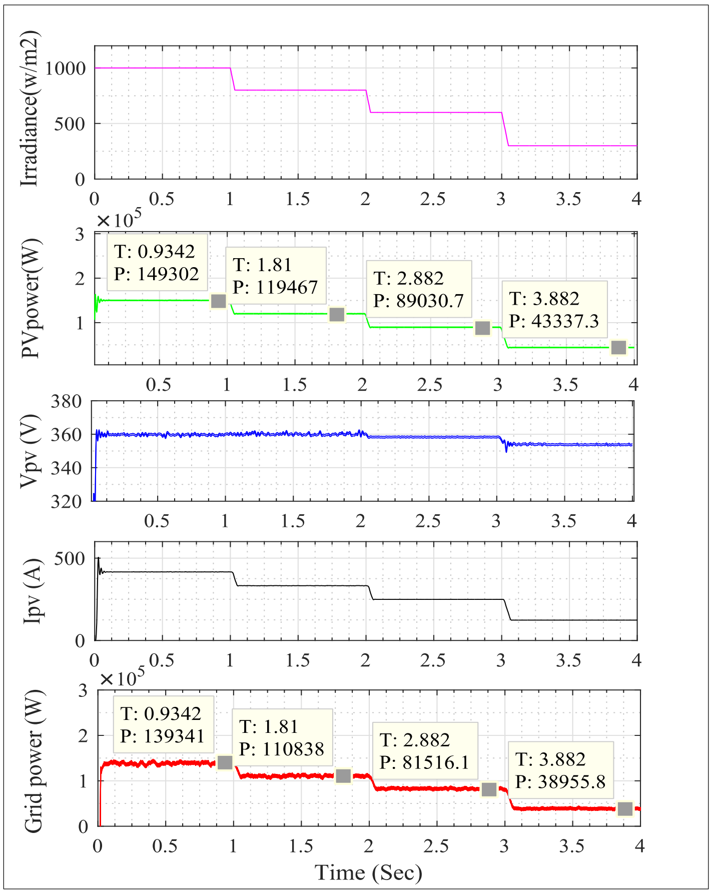

Figure 12: Two-stage topologies Simulation result.
Source: Authors, (2026).

The simulation results presented in Figures 11 and 12 illustrate key performance metrics, including voltage, current, and power output for the PV array, as well as the power injected into the grid for both single-stage and two-stage topologies. At maximum irradiance (1000 W/m²), the PV panels in the single-stage system generated an output power of 151.393 kW, with 145.643 kW successfully injected into the grid. In comparison, the two-stage system's PV panels produced a slightly lower output of 149.302 kW, of which 139.341 kW was injected into the grid due to additional conversion losses. As irradiance decreased, the single-stage topology maintained its efficiency advantage. At 800 W/m², the PV panels in the single-stage system generated 121.098 kW, with 115.405 kW reaching the grid, while the two-stage system produced 119.467 kW and injected 110.838 kW. This trend persisted at 600 W/m², with the single-stage topology producing 90.5887 kW and injecting 86.5306 kW, compared to the two-stage system's output of 89.0307 kW and grid injection of 81.5161 kW. At the lowest irradiance level (300 W/m²), the single-stage system generated 44.6634 kW, injecting 42.0708 kW into the grid, whereas the two-stage system generated 43.3373 kW with only 38.9558 kW reaching the grid.

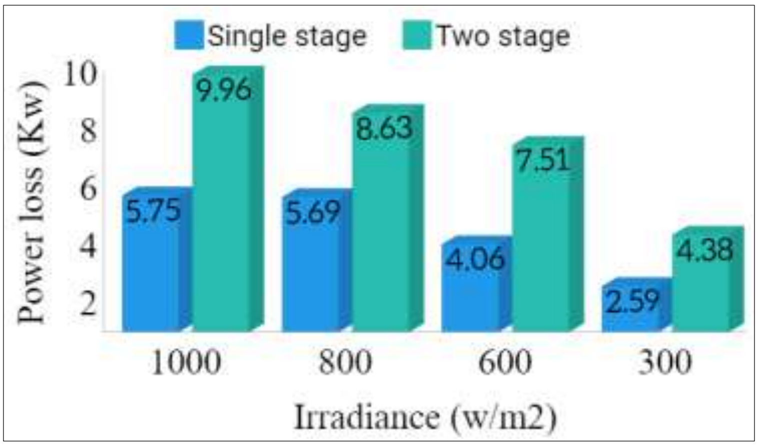

Figure 13: Quantitative Comparison of Single-Stage Two-Stage Power Losses.
Source: Authors, (2026).

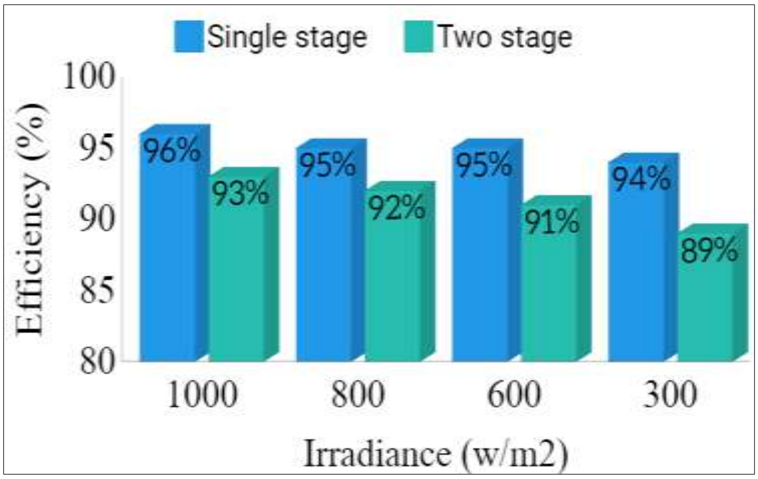

Figure 14: Quantitative Comparison of Efficiency in Single-Stage and Two-Stage Topologie.
Source: Authors, (2026).

The histogram columns in Figures 13 and 14 provide a visual, quantitative comparison between the two topologies, emphasizing the disparity in power losses at various irradiance levels. Power losses in the two-stage system reached 9.96 kW, 8.63 kW, 7.51 kW, and 4.38 kW at irradiance levels of 1000 W/m², 800 W/m², 600 W/m², and 300 W/m², respectively. In comparison, the single-stage topology showed lower losses of 5.75 kW, 5.69 kW, 4.06 kW, and 2.59 kW at the same irradiance levels. This reduction in power loss is attributed to the direct connection between the solar panels and the inverter in the single-stage design, eliminating the DC converter stage losses present in the two-stage system. The histogram effectively highlights these differences, reinforcing the efficiency advantage of the single-stage topology, which recorded efficiencies of 96%, 95%, 95%, and 94% under irradiance levels of 1000 W/m², 800 W/m², 600 W/m², and 300 W/m², respectively, as opposed to the two-stage system's efficiencies of 93%, 92%, 91%, and 89%. These results collectively support the single-stage configuration as a more efficient and economically viable choice for grid-connected PV systems, given its capacity to reduce power losses and enhance energy transfer efficiency.

VI. CONCLUSION

This study offers valuable insights into the optimisation of grid-connected photovoltaic (PV) systems through a comprehensive comparative analysis of single-stage and two-stage topologies within a 150 kW power plant framework. The findings reveal that the single-stage architecture significantly reduces power losses compared to its two-stage counterpart, resulting in enhanced overall efficiency. Furthermore, the Maximum Power Point Tracking (MPPT) algorithm exhibited superior performance in the single-stage configuration, successfully achieving a higher and more accurate maximum power point across varying solar irradiance conditions. This improvement underscores the efficacy of employing an inverter directly for maximum power tracking, as opposed to relying on a DC-

DC converter. Additionally, the single-stage topology presents multiple advantages, such as its compact size and cost-effectiveness, providing essential guidance for engineers and researchers in selecting the most optimal configurations for grid-connected PV systems.

VII. AUTHOR'S CONTRIBUTIONS

Conceptualization: Abdelmoumen Ghilani, Amel Terki, Ahmed Marouane Ghodbane, Zakaria Alili and Oussama Belaroussi.
Methodology: Abdelmoumen Ghilani, Amel Terki, Ahmed Marouane Ghodbane and Oussama Belaroussi[2]
Investigation: Abdelmoumen Ghilani, Amel Terki, Ahmed Marouane Ghodbane and Oussama Belaroussi.
Discussion of results: Abdelmoumen Ghilani, Amel Terki, Ahmed Marouane Ghodbane, Zakaria Alili and Oussama Belaroussi[2]
Writing – Original Draft: Abdelmoumen Ghilani.
Writing – Review and Editing: Abdelmoumen Ghilani and Amel Terki.
Resources: Amel Terki.
Supervision: Amel Terki, Ahmed Marouane Ghodbane, Zakaria Alili and Oussama Belaroussi.
Approval of the final text: Abdelmoumen Ghilani, Amel Terki, Ahmed Marouane Ghodbane, Zakaria Alili and Oussama Belaroussi.

VIII. REFERENCES

[1] W. V. Jahnavi and J. N. Chandra Sekhar, "A comprehensive review on application of ai algorithms for grid connected solar photovoltaic systems," Journal of Engineering and Technology for Industrial Applications, vol. 10, no. 49, pp. 87–95, Oct. 2024, doi: 10.5935/jetia.v10i49.1248.

[2] M. A. Mejias, Y. G. Landera, and L. L. Viltre, "Comparison of maximum power point tracking techniques used in photovoltaic system," Journal of Engineering and Technology for Industrial Applications, vol. 7, no. 27, pp. 4–12, Feb. 2021, doi: 10.5935/jetia.v7i27.729.

[3] Y. Houam, A. Terki, and N. Bouarroudj, "An Efficient Metaheuristic Technique to Control the Maximum Power Point of a Partially Shaded Photovoltaic System Using Crow Search Algorithm (CSA)," Journal of Electrical Engineering and Technology, vol. 16, no. 1, pp. 381–402, Jan. 2021, doi: 10.1007/s42835-020-00590-8.

[4] T. Orłowska-Kowalska, F. Blaabjerg, and J. Rodríguez, "Studies in Computational Intelligence 531 Advanced and Intelligent Control in Power Electronics and Drives." [Online]. Available: http://www.springer.com/series/7092.

[5] A. Ghilani, A. Terki, Z. Alili, A. M. Ghodbane, and O. Belaroussi, "Experimental Validation of PSO and GWO-Based MPPT for a Single-Stage Three-Phase Grid-Connected PV System Under Partial Shading," Journal Europeen des Systemes Automatises, vol. 57, no. 5, pp. 1387–1395, Oct. 2024, doi: 10.18280/jesa.570514.

[6] M. Azizi, O. Husev, and D. Vinnikov, "Single-Stage Buck–Boost Inverters: A State-of-the-Art Survey," Mar. 01, 2022, MDPI. doi: 10.3390/en15051622.

[7] A. Q. Al-Shetwi et al., "Active Power Control to Mitigate Frequency Deviations in Large-Scale Grid-Connected PV System Using Grid-Forming Single-Stage Inverters," Energies (Basel), vol. 15, no. 6, Mar. 2022, doi: 10.3390/en15062035.

[8] A. Refaat, A. E. Khalifa, M. M. Elsakka, Y. Elhenawy, A. Kalas, and M. H. Elfar, "A novel metaheuristic MPPT technique based on enhanced autonomous group Particle Swarm Optimization Algorithm to track the GMPP under partial shading conditions - Experimental validation," Energy Convers Manag, vol. 287, Jul. 2023, doi: 10.1016/j.enconman.2023.117124.

[9] M. A. Zeddini, S. Krim, and M. F. Mimouni, "Experimental validation of an advanced metaheuristic algorithm for maximum power point tracking of a shaded photovoltaic system: A comparative study between three approaches," Energy Reports, vol. 10, pp. 161–185, Nov. 2023, doi: 10.1016/j.egyr.2023.06.019.

[10] K. L. Lai, T. Thanh, and T. Tran, "Three-Phase Grid Connected Solar System With Svm Algorithm," Journal of Engineering Research and Application www.ijera.com, vol. 8, pp. 42–48, 2018, doi: 10.9790/9622-0811024248.

[11] K. Bouguerra, S. Latreche, H. Khemliche, and M. Khemliche, "Journal of Renewable Energies Comparative Study Between Synergetic Control and Sliding Mode Control using MPPT Techniques," Journal of Renewable Energies ICREPS'24 Naama, pp. 113–129, 2024, doi: 10.54966/jreen.v1i1.1281.

[12] M. H. EL-Banna, M. R. Hammad, A. I. Megahed, K. M. AboRas, A. Alkuhayli, and N. Gowtham, "On-grid optimal MPPT for fine-tuned inverter based PV system using golf optimizer considering partial shading effect," Alexandria Engineering Journal, vol. 103, pp. 180–196, Sep. 2024, doi: 10.1016/j.aej.2024.05.115.

[13] Y. Amara, R. Boukenoui, R. Bradai, and H. Salhi, "Design and Control of Two-Stage Standalone Photovoltaic Generation System," in Proceedings - International Conference on Communications and Electrical Engineering, ICCEE 2018, Institute of Electrical and Electronics Engineers Inc., Jul. 2018. doi: 10.1109/CCEE.2018.8634511.

[14] M. N. Ali, K. Mahmoud, M. Lehtonen, and M. M. F. Darwish, "An Efficient Fuzzy-Logic Based Variable-Step Incremental Conductance MPPT Method for Grid-Connected PV Systems," IEEE Access, vol. 9, pp. 26420–26430, 2021, doi: 10.1109/ACCESS.2021.3058052.

[15] V. C. Tella, B. Agili, and M. He, "Advanced MPPT Control Algorithms: A Comparative Analysis of Conventional and Intelligent Techniques with Challenges," European Journal of Electrical Engineering and Computer Science, vol. 8, no. 4, pp. 6–20, Jul. 2024, doi: 10.24018/ejece.2024.8.4.623.

[16] A. Asnil, R. Nazir, K. Krismadinata, and M. N. Sonni, "Performance Analysis of an Incremental Conductance MPPT Algorithm for Photovoltaic Systems Under Rapid Irradiance Changes," TEM Journal, vol. 13, no. 2, pp. 1087–1094, May 2024, doi: 10.18421/TEM132-23.

[17] A. Q. Al-Shetwi, M. Z. Sujod, M. A. Hannan, M. A. Abdullahd, A. S. Al-Ogaili, and K. P. Jern, "Impact of Inverter Controller-Based Grid-Connected PV System in the Power Quality," International Journal of Electrical and Electronic Engineering and Telecommunications, vol. 9, no. 6, pp. 462–469, Nov. 2020, doi: 10.18178/IJEETC.9.6.462-469.

[18] M. Mirmohammad and S. P. Azad, "Control and Stability of Grid-Forming Inverters: A Comprehensive Review," Jul. 01, 2024, Multidisciplinary Digital Publishing Institute (MDPI). doi: 10.3390/en17133186.

[19] R. Luhtala, H. Alenius, and T. Roinila, "Practical implementation of adaptive SRF-PLL for three-phase inverters based on sensitivity function and real-time grid-impedance measurements," Energies (Basel), vol. 13, no. 5, Mar. 2020, doi: 10.3390/en13051173.

[20] I. Jamal, M. F. Elmorshedy, S. M. Dabour, E. M. Rashad, W. Xu, and D. J. Almakhles, "A Comprehensive Review of Grid-Connected PV Systems Based on Impedance Source Inverter," IEEE Access, vol. 10, pp. 89101–89123, 2022, doi: 10.1109/ACCESS.2022.3200681.